Taylor & Francis
Taylor & Francis Group

Numerical Heat Transfer, Part A: Applications
An International Journal of Computation and Methodology

ISSN: (Print) (Online) Journal homepage: https://www.tandfonline.com/loi/unht20

Derivation of a continuous adjoint topology optimization method applied on heat transfer for incompressible flow

Yi Ye, Xueying Li, Jing Ren & Bengt Sundén

To cite this article: Yi Ye, Xueying Li, Jing Ren & Bengt Sundén (2022): Derivation of a continuous adjoint topology optimization method applied on heat transfer for incompressible flow, Numerical Heat Transfer, Part A: Applications, DOI: 10.1080/10407782.2022.2102348

To link to this article: https://doi.org/10.1080/10407782.2022.2102348

Published online: 27 Jul 2022.

NUMERICAL HEAT TRANSFER, PART A: APPLICATIONS
https://doi.org/10.1080/10407782.2022.2102348

Taylor & Francis
Taylor & Francis Group

OPEN ACCESS Check for updates

Derivation of a continuous adjoint topology optimization method applied on heat transfer for incompressible flow

Yi Ye[a], Xueying Li[a], Jing Ren[a], and Bengt Sundén[b]

[a]Tsinghua University, Beijing, P.R. China; [b]Department of Energy Sciences, Lund University, Skåne, Sweden

ABSTRACT
With the development of additive manufacturing, the freedom in developing complex cooling structures has been enlarged greatly. Topology optimization is one of the methods that can give out cooling structures beyond the limits of geometric parameters. In this research, an algorithm of topology optimization with heat transfer is derived. The detailed optimization procedure is presented in this work. The basic assumptions of this optimization method are steady state, incompressible and frozen turbulent flow with constant physical properties. The governing equations, optimization sensitivity formula and boundary conditions are presented, which are essential to the implementation of this method. A detailed derivation process is included. This method is applied in a 2-D flow domain using an open-source platform named OpenFOAM.

ARTICLE HISTORY
Received 26 February 2022
Accepted 11 July 2022

KEYWORDS
Continuous adjoint method; heat transfer; topology optimization

1. Introduction

Gas turbine is one of the most efficient energy utilization patterns, which is widely used in power plants, aircraft engines and navigation. The turbine inlet temperature is an essential parameter for efficiency, which has reached values far beyond the allowable temperature for the material of turbine blade. Enormous efforts have been made to find new materials and develop new cooling techniques over decades. The conventional cooling structure design procedure is based on geometric parameters of typical cooling structures such as serpentine channel, pin-fin and ribs which are developed through experiments and numerical simulations. Engineers must obtain a broad knowledge before the procedure of cooling structure design. However, the conventional design concept may slow down the speed of developing new cooling structures, since parametric description will constrain searching space of cooling design. Some novel structure doesn't have regular shape that can be described using geometric parameters.

Topology Optimization is one of the methods that may make a break through beyond the existing parametric design procedure. Topology Optimization was proposed by Bendsoe and Kikuchi [1] in 1988. Then, Bendsoe and Sigmud gave a systematic introduction of this technique [2]. For a long time, Topology Optimization was only applied in structure mechanics design such as bridge construction and buildings. In the beginning of the topological optimization realization, a design domain fulfilled with solid material is provided, there is no specific structure. By applying load on the domain, the mechanical stress can be evaluated. Then, areas with low stress will

CONTACT Bengt Sundén bengt.sunden@energy.lth.se Division of Heat Transfer, P.O. Box 118, Department of Energy Sciences, Lund University, Lund, Skåne, SE-22100 Sweden.

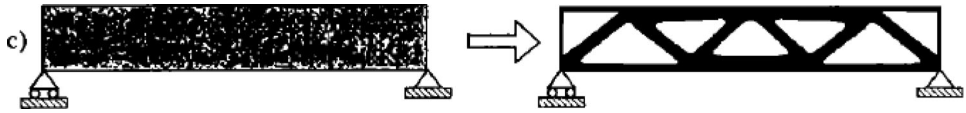

Figure 1. Topology optimization applied in structural design [2].

be weakened by arranging lower density. It delivers an un-biased design from scratch that automatically fulfilling the domain constraints. The approach is shown in Figure 1.

It took more than 10 years for this elegant concept to enter the research field of fluid dynamics. Borrvall and Petersson [3] and Klimetzek [4] performed topological optimization methods for duct flows independently. Their ideas are similar to the topological method used in structure mechanics. The method starts from a domain filled with uniform porous material. Then "counter-productive" cells are identified and the counter-productive cells with lower porosity are punished. Figure 2 gives a brief introduction of this concept.

To extend this method toward three-dimensional flows, a Darcy porosity term $-\alpha v$ was introduced into the momentum equation by Gersborg-Hansen [6] and Othmer [7]. In 2008 Othmer [8] published an article introducing Topology Optimization using a continuous adjoint method. He also provided a detailed derivation process, which contributed a lot to the development of Topology Optimization in fluid dynamics. To simplify the numerical approach, an assumption named "frozen turbulence" was introduced which neglecting the variation of the eddy viscosity [9].

However, it took more time for this concept to enter the fields of heat transfer. Dede [10] conducted research to minimize the mean temperature and flow power dissipation in a flat plate heated uniformly. He solved the equations using COMSOL. In 2013, Kontoleontos [11] performed adjoint based constrained topology for viscous flows concerning heat transfer. He provided the detailed derivation process, governing equations, optimization sensitivity and boundary conditions. However, his work cares more about the heat transfer result of the fluid, conjugate phenomena were not considered yet. Matsumori [12] proposed a method which can model both solid and fluid parts simultaneously using a single governing equation. Marck and Alexandersen [13] introduced a variable thermal diffusivity as an interpolation between the solid and fluid areas using design variables. Gilles Marck [14] published an article about Topology Optimization of heat transfer in laminar flow. In his article, many critical information about this method is discussed, including optimization loop, finite-volume method and multiobjective optimization setting and method of moving asymptotes.

In 2016, Pietropaoli [15] performed a topological optimization approach for typical internal cooling of gas turbines. In his work, U-bend and narrow channel were optimized. Constant temperature boundary condition was applied on the side wall and no heat source existed within the domain. The cost function he introduced is a multiobject function. But adjoint governing equation, optimization sensitivity and adjoint boundary condition were not provided.

In this work, a detailed deviation of a continuous adjoint based topology optimization method concerning heat transfer for a gas turbine internal cooling case is provided. The governing equation, optimization sensitivity and boundary condition which are essential to perform this method are provided. The basic assumption of this study is steady state, incompressible, frozen turbulence flow with constant physical properties. This method is applied in a 2-D flow domain.

2. Description of optimization problem

The approach to find a better heat transfer structure of a gas turbine blade is a typical optimization problem under constraints. The objective function which is also known as cost function J has various forms, such as total heat transfer across the domain, total pressure dissipation and velocity uniformity at the outlet. A multiobjective optimization could use the combination of these cost functions. In our case, we chose heat transfer and total pressure dissipation as the

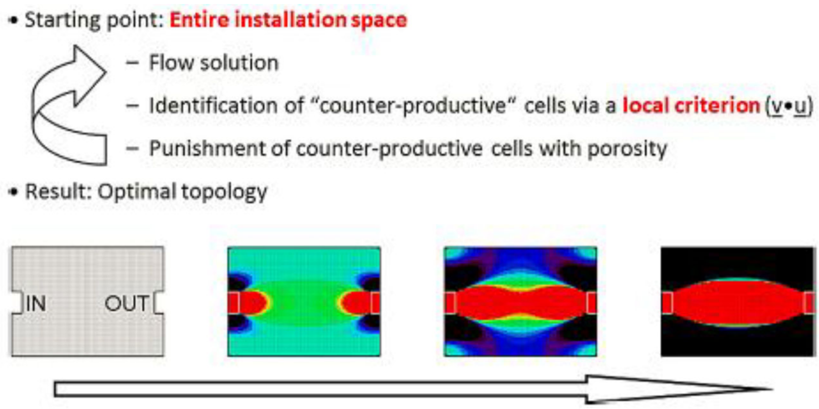

Figure 2. The principle of CFD topology optimization [5].

objectives of optimization. The cost function is shown below. This function is same as the one in

$$J = -\varphi_1 \int_\Gamma d\Gamma \left(p + \frac{1}{2} v^2 \right) v \cdot n - \varphi_2 \int_\Gamma d\Gamma (Tv \cdot n) \tag{1}$$

φ_1 and φ_2 are weight factors representing the different contributions of total pressure dissipation and heat transfer to the cost function. As can be seen from the formula, the objective function is an integral of the boundary, which has no contribution from the internal domain. Other formulations could take the internal portion into account, such as the mean temperature across the domain, see Sumer [16].

The cost function J is a function of flow velocity v, pressure p and temperature T which are the state parameters of the flow domain. Navier-Stokes equation, energy equation and geometric boundary are constraints for this optimization problem.

The crucial idea of the Topology Optimization is to find a way to substitute the structure parametric design procedure. To accomplish this goal, the topology optimization formulates its approach based on a porous assumption. A design variable assigned as α is included, which has a range from zero to a maximum value. The objective domain is initialized uniformly overall without discrimination of solid and fluid parts. The momentum equation is shown below:

$$(v \cdot \nabla)v + \nabla p - \nabla \cdot \left(\upsilon \left(\nabla v + (\nabla v)^T \right) \right) + \alpha v = 0 \tag{2}$$

The last term on the left side is called the Darcy term. It introduces a resistance force against flow field. The distribution of α indicates different resistance to flow field. In the areas where the value of α is high, the velocity is reduced to zero, which indicates solid portion. In the position where α equals zero, the momentum equation has the same form as the normal Navier-Stokes equation, which indicates fluid portion. The α is the only design variable of this method.

The solid and fluid parts have different thermal diffusion coefficient. The temperature equation is shown below [15].

$$v \cdot \nabla T - \nabla \cdot (k(\alpha) \nabla T) = 0 \tag{3}$$

In the area where α is pretty high, the velocity is close to zero. So the first term of Eq. (3) in the left will vanish. This problem is reduced into a heat conduction problem.

There are many different forms to define the variation of α and thermal diffusion coefficient k. In this article, we chose the equation illustrated by M. Pietropaoli [15], which is shown below.

$$k(\alpha) = \frac{\gamma(\alpha)\left(k_f(1+\eta) - k_s\right) + k_s}{1 + \eta\gamma(\alpha)} \tag{4}$$

$$\gamma(\alpha) = \left(1 - \frac{\alpha}{\alpha_{max}}\right)^{\lambda} \tag{5}$$

The k_s and k_f are thermal diffusivity of solid and fluid materials. $\gamma(\alpha)$ represents the influence of α on $\mathrm{k}(\alpha)$. λ and η are real constant used to tune the convexity of the function.

Then the optimization problem can be summarized as follows:

$$\text{Minimize } \mathrm{J} = \mathrm{J}(\alpha, \mathrm{v}, \mathrm{p}, \mathrm{T}) \tag{6}$$

$$\text{subject to } \mathrm{R}(\alpha, \mathrm{v}, \mathrm{p}, \mathrm{T}) = 0$$

R stands for the constraints of the optimization problem. Navier-Stokes equation and temperature equation are the main constraints for this problem. The constraints are summarized as follows:

$$R_v = (\mathrm{v} \cdot \nabla)\mathrm{v} + \nabla \mathrm{p} - \nabla \cdot \left(\upsilon\left(\nabla \mathrm{v} + (\nabla \mathrm{v})^T\right)\right) + \alpha \mathrm{v} \tag{6}$$

$$R_P = -\nabla \cdot \mathrm{v} \tag{7}$$

$$R_T = \mathrm{v} \cdot \nabla \mathrm{T} - \nabla \cdot (\mathrm{k}(\alpha)\nabla \mathrm{T}) \tag{8}$$

The above constraints and objective cost function has the similar formulation as Pietropaoli [15].

The goal of topology optimization procedure is to find a distribution of α which can minimize cost function J. Since the number of design variable α_i equals the number of vortex for the mesh, it is impossible to solve α though direct optimization approach. The most difficult issue of this optimization method is the calculation of optimization sensitivity $\frac{\partial J}{\partial \alpha_i}$, which is also known as the gradient of α_i on cost function.

3. Continuous adjoint method

To calculate the sensitivity, a method called adjoint approach is conducted. There are two types of adjoint approach commonly used in Topology Optimization. One is called discrete adjoint approach, which requires to rewrite the CFD solver. Details about discrete adjoint approach can be found in the work of Gilles Marck [14]. In this article continuous adjoint approach is utilized, which is easy to perform in open source CFD software. The fundamental thought of this method is called Lagrange multiplier, which combine cost function and constraints function into one object function.

$$\mathrm{L} = \mathrm{J} + \int_{\Omega} uR_v d\Omega + \int_{\Omega} qR_p d\Omega + \int_{\Omega} tR_T d\Omega \tag{9}$$

In which Ω refers to flow domain. $(u, q, t) = (u_1, u_2, u_3, q, t)$ are Lagrange multipliers. We call them adjoint velocity u, adjoint pressure q and adjoint temperature t. They are introduced as virtual variables to conduct adjoint method, which means they have no actual physical meanings.

The optimum result can only be reached under the following conditions, which can be proved mathematically.

$$\frac{\partial \mathrm{L}}{\partial \mathrm{v}} = \frac{\partial \mathrm{L}}{\partial \mathrm{p}} = \frac{\partial \mathrm{L}}{\partial \mathrm{T}} = \frac{\partial \mathrm{L}}{\partial \alpha} = 0 \tag{10}$$

$$\frac{\partial \mathrm{L}}{\partial \mathrm{u}} = \frac{\partial \mathrm{L}}{\partial \mathrm{q}} = \frac{\partial \mathrm{L}}{\partial \mathrm{t}} = 0 \tag{11}$$

3.1. Derivation of state equations and boundary conditions for the continuous adjoint method

Equations (9)–(11) are the foundations of the continuous adjoint method. The logic of this method is to solve Eqs. (10) and (11) to get optimum distribution of α.

The cost function J has no influence from the adjoint parameters u, q, t. Then, Eq. (11) can be simplified into the form shown below:

$$\int_\Omega R_v d\Omega = \int_\Omega R_p d\Omega = \int_\Omega R_T d\Omega = 0 \tag{12}$$

Then we will get

$$R_v = R_p = R_T = 0 \tag{13}$$

This is a typical computational fluid dynamics problem. These equations can be solved by a computational fluid dynamics program using SIMPLE loop.

Next, reformulate Eq. (10) into differential form.

$$\delta_\alpha L = \delta_v L = \delta_p L = \delta_T L = 0 \tag{14}$$

By expending Eq. (14) we will get the following equations:

$$\delta_v L = \delta_v J + \int_\Omega u \delta_v R_v d\Omega + \int_\Omega q \delta_v R_p d\Omega + \int_\Omega t \delta_v R_T d\Omega = 0 \tag{15}$$

$$\delta_p L = \delta_p J + \int_\Omega u \delta_p R_v d\Omega + \int_\Omega q \delta_p R_p d\Omega + \int_\Omega t \delta_p R_T d\Omega = 0 \tag{16}$$

$$\delta_t L = \delta_t J + \int_\Omega u \delta_t R_v d\Omega + \int_\Omega q \delta_t R_p d\Omega + \int_\Omega t \delta_t R_T d\Omega = 0 \tag{17}$$

$\delta_p R_v$ is the differential of R_v with respect to the variation of pressure p. The forms of these are summarized below:

$$\delta_v R_v = (\delta \mathrm{v} \cdot \nabla)\mathrm{v} + (\mathrm{v} \cdot \nabla)\delta \mathrm{v} - \nabla \cdot \left(\upsilon \left(\nabla \delta \mathrm{v} + (\nabla \delta \mathrm{v})^T \right) \right) + \alpha \delta \mathrm{v} \tag{18}$$

$$\delta_v R_p = -\nabla \cdot \delta \mathrm{v} \tag{19}$$

$$\delta_v R_T = \delta \mathrm{v} \cdot \nabla \mathrm{T} \tag{20}$$

$$\delta_p R_v = \nabla \delta p \tag{21}$$

$$\delta_p R_P = 0 \tag{22}$$

$$\delta_p R_T = 0 \tag{23}$$

$$\delta_T R_v = 0 \tag{24}$$

$$\delta_T R_P = 0 \tag{25}$$

$$\delta_T R_T = \mathrm{v} \cdot \nabla \delta \mathrm{T} - \nabla \cdot (\mathrm{k}(\alpha) \nabla \delta \mathrm{T}) \tag{26}$$

The differential of the cost function $\delta_v J$ can be divided into the integral at the boundary and internal domain as shown below:

$$\delta_v J = \int_\Omega d\Omega \frac{\partial J_\Omega}{\partial v} \delta v + \int_\Gamma d\Gamma \frac{\partial J_\Gamma}{\partial v} \delta v \tag{27}$$

Then Eqs. (15)–(17) can be derived into the form below:

$$\begin{aligned} \delta_v L = & \int_\Gamma d\Gamma \left(\mathrm{n}(\mathrm{u} \cdot \mathrm{v}) + \mathrm{u}(\mathrm{v} \cdot \mathrm{n}) + 2\nu \mathrm{n} \cdot \mathrm{D}(\mathrm{u}) - \mathrm{qn} + \frac{\partial J_\Gamma}{\partial v} \right) \cdot \delta v - \int_\Gamma d\Gamma 2\nu \mathrm{n} \cdot \mathrm{D}(\delta \mathrm{v}) \cdot \mathrm{u} \\ & + \int_\Omega d\Omega \left(-\nabla \mathrm{u} \cdot \mathrm{v} - (\mathrm{v} \cdot \nabla)\mathrm{u} - \nabla \cdot (2\nu \mathrm{D}(\mathrm{u})) + \alpha \mathrm{u} + \nabla \mathrm{q} + \frac{\partial J_\Omega}{\partial v} + t \nabla \mathrm{T} \right) \cdot \delta v = 0 \end{aligned} \tag{28}$$

$$\delta_p L = \int_\Gamma d\Gamma\left(\mathbf{u}\cdot \mathrm{n} + \frac{\partial J_\Gamma}{\partial p}\right)\delta p + \int_\Omega d\Omega\left(-\nabla\cdot \mathrm{u} + \frac{\partial J_\Omega}{\partial p}\right)\delta p = 0 \tag{29}$$

$$\begin{aligned}\delta_t L = &\int_\Gamma d\Gamma\left(\mathrm{tv}\cdot \mathrm{n} - \mathrm{t}\nabla \mathrm{k}(\alpha)\cdot \mathrm{n} + 2\nabla(\mathrm{tk}(\alpha))\cdot \mathrm{n} + \frac{\partial J_\Gamma}{\partial T}\right)\delta T\\ &+ \int_\Omega d\Omega\left(-\mathrm{v}\cdot\nabla(\mathrm{t}) - \mathrm{t}\nabla\cdot \mathrm{v} + \nabla \mathrm{k}(\alpha)\cdot\nabla \mathrm{t} + \mathrm{t}\nabla^2 \mathrm{k}(\alpha) - \nabla^2(\mathrm{tk}(\alpha)) + \frac{\partial J_\Omega}{\partial T}\right)\delta T\\ &- \int_\Gamma d\Gamma\nabla(\mathrm{tk}(\alpha)\delta \mathrm{T})\cdot \mathrm{n} = 0\end{aligned} \tag{30}$$

The deviation of Eqs. (28) and (29) can be found in the work by Othmer [8]. The only difference is the last term of Eq. (28), by which the temperature is conjugated with the momentum equation. The result is divided into two parts.

First, the adjoint equations:

$$-\nabla \mathrm{u}\cdot \mathrm{v} - (\mathrm{v}\cdot\nabla)\mathrm{u} = -\nabla \mathrm{q} + \nabla\cdot\left(\upsilon\left(\nabla \mathrm{u} + (\nabla \mathrm{u})^T\right)\right) - \alpha \mathrm{u} - t\nabla \mathrm{T} - \frac{\partial J_\Omega}{\partial v} \tag{31}$$

$$\nabla\cdot \mathrm{u} = \frac{\partial J_\Omega}{\partial p} \tag{32}$$

Second, the adjoint boundary conditions.

$$\int_\Gamma d\Gamma\left(\mathrm{n}(\mathrm{u}\cdot \mathrm{v}) + \mathrm{u}(\mathrm{v}\cdot \mathrm{n}) + 2\nu \mathrm{n}\cdot \mathrm{D}(\mathrm{u}) - \mathrm{qn} + \frac{\partial J_\Gamma}{\partial v}\right)\cdot\delta v - \int_\Gamma d\Gamma 2\nu \mathrm{n}\cdot \mathrm{D}(\delta \mathrm{v})\cdot \mathrm{u} = 0 \tag{33}$$

$$\int_\Gamma d\Gamma\left(\mathbf{u}\cdot \mathrm{n} + \frac{\partial J_\Gamma}{\partial p}\right)\delta p = 0 \tag{34}$$

Equation (30) has to be fulfilled for any δT that happens in the interior of flow domain. So the second term of Eq. (30), which is integral of internal flow domain, has to vanish. Then we get Eq. (35). This is the state equation for the adjoint temperature.

$$-\mathrm{v}\cdot\nabla(\mathrm{t}) - \mathrm{t}\nabla\cdot \mathrm{v} + \nabla \mathrm{k}(\alpha)\cdot\nabla \mathrm{t} + \mathrm{t}\nabla^2 \mathrm{k}(\alpha) - \nabla^2(\mathrm{tk}(\alpha)) + \frac{\partial J_\Omega}{\partial T} = 0 \tag{35}$$

The adjoint boundary condition for temperature results from the integrals over the boundary of Eq. (30).

$$\int_\Gamma d\Gamma\left(\mathrm{tv}\cdot \mathrm{n} - \mathrm{t}\nabla \mathrm{k}(\alpha)\cdot \mathrm{n} + 2\nabla(\mathrm{tk}(\alpha))\cdot \mathrm{n} + \frac{\partial J_\Gamma}{\partial T}\right)\delta T - \int_\Gamma d\Gamma\nabla(\mathrm{tk}(\alpha)\delta \mathrm{T})\cdot \mathrm{n} = 0 \tag{36}$$

3.2. Specialization to duct flows

We take duct flow as the physical model to specialize the topology optimization, because the internal cooling channels of a turbine vane and blade can be simplified into a duct flow. The cost function only contains the integrals over the inlet and outlet. So the differential of the cost functions w.r.t v, p and T over the internal domain disappears. Then the adjoint state equations can be reformulated as follows:

$$-\nabla \mathrm{u}\cdot \mathrm{v} - (\mathrm{v}\cdot\nabla)\mathrm{u} = -\nabla \mathrm{q} + \nabla\cdot\left(\upsilon\left(\nabla \mathrm{u} + (\nabla \mathrm{u})^T\right)\right) - \alpha \mathrm{u} - t\nabla \mathrm{T} \tag{37}$$

$$\nabla\cdot \mathrm{u} = 0 \tag{38}$$

$$-\mathrm{v}\cdot\nabla \mathrm{t} - \nabla\cdot(\mathrm{k}(\alpha)\nabla \mathrm{t}) = 0 \tag{39}$$

The adjoint boundary conditions need to be specified for each edge. The specialization of the boundary for the adjoint velocity and adjoint pressure can be found in the literature by Othmer [8]. The specialization for the adjoint temperature condition is performed here.

Because the temperatures of the wall and inlet are prescribed, the variation of temperature δT equals zero. The temperature of the outlet was zero-gradient, which means $\nabla(\delta \mathrm{T})$ equals zero.

For the inlet and wall, Eq. (36) can be simplified as follows:

$$\nabla(\mathrm{tk}(\alpha)\delta\mathrm{T})\cdot\mathrm{n} = \mathrm{tk}(\alpha)\nabla(\delta\mathrm{T})\cdot\mathrm{n} + \delta\mathrm{Tk}(\alpha)\nabla\mathrm{t}\cdot\mathrm{n} + \delta\mathrm{Tt}\nabla(\mathrm{k}(\alpha))\cdot\mathrm{n} = 0 \tag{40}$$

Since $\delta T = 0,$ we can get the following condition at inlet.

$$\mathrm{t} = 0 \tag{41}$$

For the outlet, $\nabla(\delta\mathrm{T})$=0. Equation (40) can be simplified as follows:

$$\mathrm{tv}\cdot\mathrm{n} - \mathrm{t}\nabla\mathrm{k}(\alpha)\cdot\mathrm{n} + 2\mathrm{t}\nabla(\mathrm{k}(\alpha))\cdot\mathrm{n} + 2\mathrm{k}(\alpha)\nabla\mathrm{t}\cdot\mathrm{n} - \mathrm{t}\nabla\mathrm{k}(\alpha)\cdot\mathrm{n} - \mathrm{k}(\alpha)\nabla\mathrm{t}\cdot\mathrm{n} + \frac{\partial J_\Gamma}{\partial T} = 0 \tag{42}$$

In this article the cost function has the form below.

$$\mathrm{J} = -\varphi_1\int_\Gamma \mathrm{d}\Gamma\left(\mathrm{p} + \frac{1}{2}\mathrm{v}^2\right)\mathrm{v}\cdot\mathrm{n} - \varphi_2\int_\Gamma \mathrm{d}\Gamma(\mathrm{Tv}\cdot\mathrm{n}) \tag{43}$$

Then we can get the differentiations of cost function.

$$\frac{\partial J_\Gamma}{\partial p} = -\varphi_1\mathrm{v_n} \tag{44}$$

$$\frac{\partial J_\Gamma}{\partial v_n} = -\varphi_1\left(\frac{1}{2}v_t^2 + \frac{3}{2}v^2\right) - \varphi_2 T \tag{45}$$

$$\frac{\partial J_\Gamma}{\partial v_t} = -\varphi_1\mathrm{v_n v_t} \tag{46}$$

$$\frac{\partial J_\Gamma}{\partial T} = -\varphi_2\mathrm{v_n} \tag{47}$$

We will get the final form of the adjoint boundary condition as follows:

Adjoint boundary condition for the wall and inlet:

$$u_t = 0 \tag{48}$$

$$u_n = \varphi_1\mathrm{v_n} \tag{49}$$

$$\mathrm{t} = 0 \tag{50}$$

Adjoint pressure has the same type of boundary condition as the prime pressure at the inlet and wall.

Adjoint boundary condition for the outlet:

$$\mathrm{q} = \mathrm{u}\cdot\mathrm{v} + u_n v_n + \nu(\mathrm{n}\cdot\nabla)u_n - \varphi_1\left(\frac{1}{2}v_t^2 + \frac{3}{2}v^2\right) - \varphi_2 T \tag{51}$$

$$0 = v_n u_t + \nu(\mathrm{n}\cdot\nabla)u_t - \varphi_1\mathrm{v_n v_t} \tag{52}$$

$$\mathrm{tv}\cdot\mathrm{n} + \mathrm{k}(\alpha)\nabla\mathrm{t}\cdot\mathrm{n} - \varphi_2\mathrm{v_n} = 0 \tag{53}$$

Now the only problem unsolved is $\delta_\alpha L = 0$.

To get the optimum α a steepest decent method is used.

The sensitivity of α is shown below, which can be drawn by a direct differentiation.

$$\frac{\partial \mathrm{L}}{\partial \alpha_i} = \left[\mathrm{u} \cdot \mathrm{v} + \mathrm{t}\left(-\nabla \cdot \left(\frac{\partial \mathrm{k}(\alpha)}{\partial \alpha_i} \nabla \mathrm{T} \right) \right) \right] \cdot V_i \tag{54}$$

The optimization procedures are summarized as follows.

(1) Give an initial distribution of α and solve Eq. (13), which is a typical computational fluid dynamics approach.
(2) Solve adjoint state equation using updated primal state parameters. In this article adjoint state equation are Eqs. (37)–(39).
(3) Calculate optimization sensitivity $\frac{\partial \mathrm{L}}{\partial \alpha}$, using Eq. (54).

V_i represents the volume of mesh element. It worth noting that V_i varies through the domain, since the mesh will is denser in regions close to wall. In this article, V_i are prescribed to be constant to eliminate the influence of the size of cells.

(4) Update α using optimization loop such as simulated annealing.
(5) Repeat step (1) to (4).

In this study steepest method is used to update α. Other optimization loop such as the method of moving asymptotes developed by Svanberg [17] can also be used.

The optimization procedure is solved using an open source platform called OpenFOAM. The solver for heat transfer can be modified from existing solver adjointShapeOptimization which only apply Topology Optimization in fluid dynamics without heat transfer. The form of adjoint state equations have the same form as primal state equations. They are both solved through a SIMPLE loop.

The boundary conditions for primal state equation are summarized as below:

- For temperature T, Dirichlet condition is applied at the inlet and the walls. Neumann condition is applied at the outlet. The inlet temperature is lower than that of wall temperature.
- For velocity v, Dirichlet condition is applied at the inlet, no-slips condition is applied at the walls, and Neumann condition is applied at the outlet.
- For pressure p, Dirichlet condition is applied at the outlet. Neumann condition is applied at the inlet.
- For design variable α, its value is fixed at zero for all boundaries.

The boundary conditions for adjoint state equation are summarized as follows:

- For inlet and wall, boundary conditions are Eqs. (48)–(50).
  The adjoint pressure q has the same type of condition of primal pressure p at the inlet and the walls. The subscript n and t indicate normal and tangential components.
- For outlet, boundary conditions are Eqs. (51)–(53).

As can be seen, the form of boundary condition for adjoint state equation is different from the primal one. That means the new boundary condition has to be coded individually in OpenFOAM.

4. Topology optimization of internal cooling

To show this method much more clearly, we perform this method in a 2-D domain as shown in Figure 3. It is a reducing pipe with a back step.

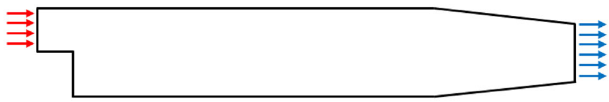

Figure 3. Flow domain sketch.

Table 1. Weight factors.

CASE ID	φ_1	φ_2
1	1	0
2	0.5	0.5
3	0.2	0.8

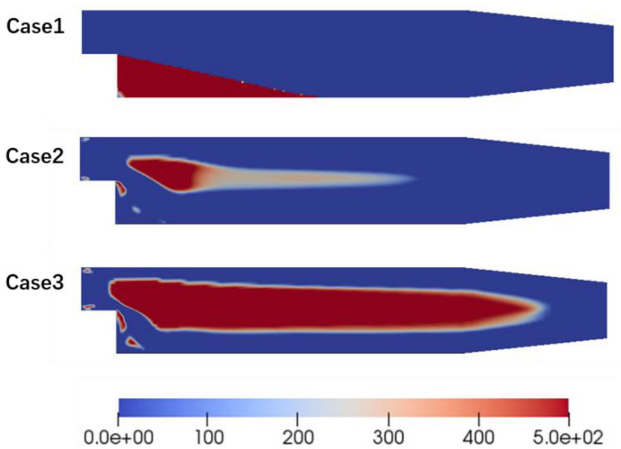

Figure 4. Geometries of optimized results.

Red arrows indicate inlet boundary. Blue arrows indicate outlet boundary. The other patches are wall boundary. Inlet velocity is 6 m/s with a fixed temperature 800 K. The temperature of wall is much higher in order to heat the flow, which is 1,800 K. Three different pairs of weight factor are chosen in this study, which are summarized below in Table 1. Case 3 has the highest weight factor for heat transfer. Thermal diffusivity of solid is $3.13 \times 10^{-6}\ m^2/s$ which is kept the same of Inconel. The thermal diffusivity of coolant is $1.18 \times 10^{-4}\ m^2/s$. The kinematic viscosity of coolant is $7.6 \times 10^{-5}\ m^2/s$. The upper limit of α is chosen to be 500.

It worth noting that the value of thermal diffusivity $k(\alpha)$ for wall boundaries is kept the same as the core value of adjacent internal cells when finite volume method is used.

5. Results

Figure 4 shows the optimization results of the three cases. The region has the color of red means solid portion. Blue area indicates fluid. Case 1, which only optimizes the total pressure dissipation, the step of the initial geometry is smoothed by an inclined line. This result coincides with our common knowledge that the step is the main cause of vortex and total pressure dissipation. This result also provides an instruction on the angel of this inclined line. Case 2 and case 3 have the similar shape. There are diversion body generate within the domain, which is used to force the flow closer to high temperature wall at the same time accelerate the speed of flow. The size of diversion body in case 3 is bigger than case 2, which will result in higher heat transfer.

The velocity contour of this case is shown in Figure 5. It’s clear to see that, the majority of coolant for case 3 is forced to move close to high temperature walls, and have higher velocity

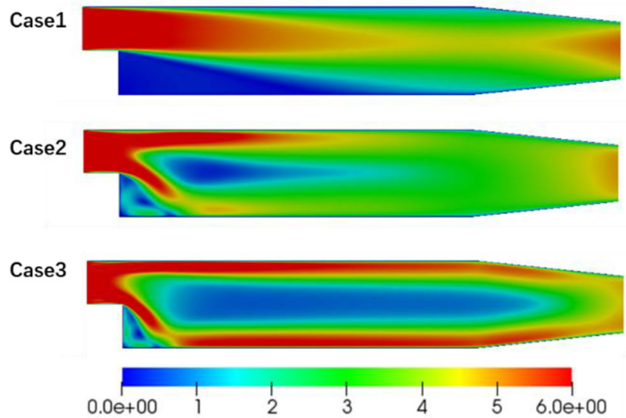

Figure 5. Velocity distributions for all cases.

Table 2. Optimization results.

Case ID	Power dissipation	Heat transfer	Cost function
1	1.03×10^{-3}	2.03×10^{-2}	1.03×10^{-3}
2	4.82×10^{-3}	2.77×10^{-2}	-1.15×10^{-2}
3	1.58×10^{-2}	3.33×10^{-2}	-2.35×10^{-2}

compared with case 2. The two branches of coolant flow will cool both upper and lower walls. Case 2 has the similar velocity distribution with case 3, but with lower velocity, as a result lower heat transfer.

The final value of the cost function is summarized in Table 2. It's clear to see case 1 has the lowest total pressure dissipation and heat transfer at the same time. The heat transfer result of case 2 has increased 40% compared with case 1. Case 3 has the highest heat transfer result which is 67% higher than case 1. The total pressure dissipation of case 3 is also the highest, which is almost 15 times that of case 1. This comparison is much more clear in Figure 6.

5.1. Abnormal distribution of adjoint temperature

There are some small spots in the inlet region of Case 2 and Case 3, which can be seen more clearly in Figure 7.

The abnormal distribution of adjoint temperature t is the main cause of the emergence of these spots. As shown in Figure 8, the values of adjoint temperature t at the vertices of the first layer after inlet are more than 10 times the values of the main body. The values of adjoint temperature t at vertices of the main body are below 0.8.

From Eq. (14) we can find that adjoint temperature is conjugated with adjoint velocity. The abnormal distribution of adjoint temperature t results in an abnormal distribution of adjoint velocity u at the inlet, as shown in Figure 9. There are two areas with high value in the inlet of the domain. And these regions coincide with the places of small spots found in Figure 7.

It can be figure out from Eq. (16) that the information of adjoint temperature t propagates from outlet to inlet which is backward with the temperature T. The boundary condition of adjoint temperature t at inlet is a fixed value. These two factors lead to the uneven distribution of adjoint temperature t and the emergence of spots in the inlet. When the optimization process continues, the spots may get bigger and result in a failure of this process.

One of the methods to eliminate the abnormal distribution of adjoint temperature t is changing the boundary condition of adjoint temperature t at inlet to Neumann condition. Since the

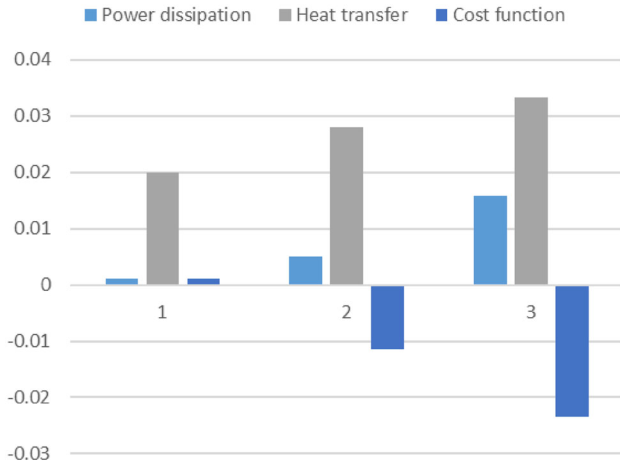

Figure 6 The value of object function for optimized results.

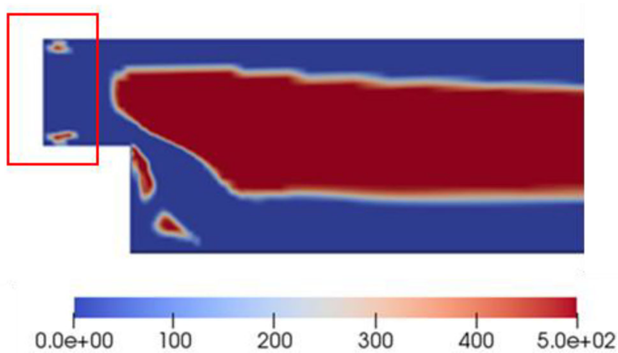

Figure 7. Small spots found in the inlet of Case 3.

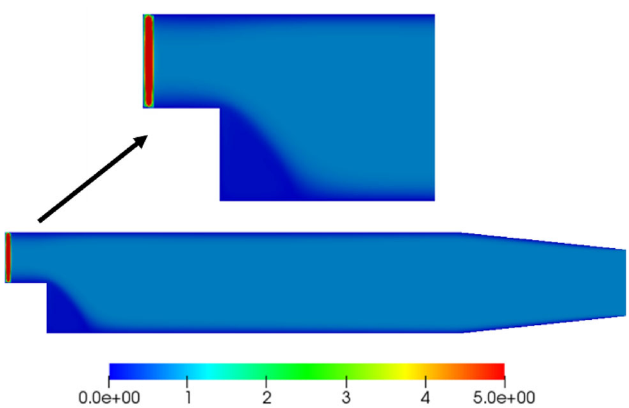

Figure 8. Distribution of adjoint temperature in Case 3.

information of adjoint temperature t is propagating backward, this modification won't influence the optimization results except for inlet area. And this method will generate a smooth inlet as shown in Figure 10.

The distribution of adjoint temperature t and adjoint velocity u is shown in Figures 11 and 12, respectively.

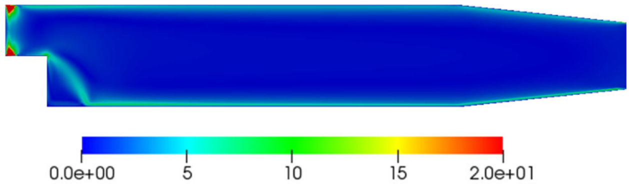

Figure 9. Distribution of adjoint velocity in Case 3.

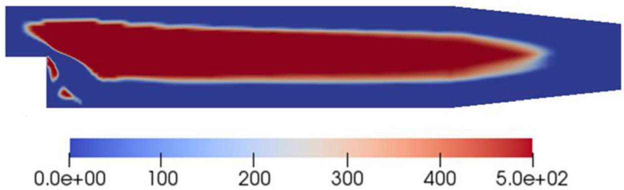

Figure 10. Geometry of the modified result.

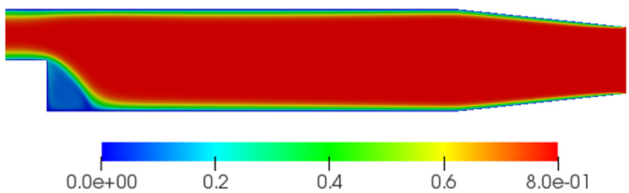

Figure 11. Distribution of adjoint temperature of the modified result.

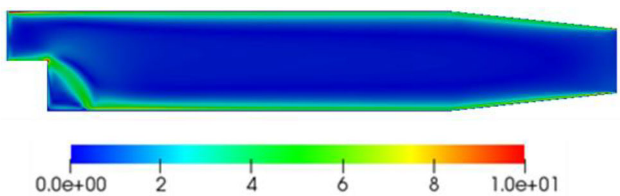

Figure 12. Distribution of adjoint velocity of the modified result.

6. Conclusions

Topology Optimization is a kind of method which will make full use of the freedom given by additive manufacturing which may provide cooling structure beyond designers' knowledge.

In this work, a detailed deviation of continuous adjoint topology optimization method about heat transfer in internal cooling case is provided based on the assumption of incompressible, frozen turbulence flow with constant physical property parameters. And governing equation, optimization sensitivity and boundary condition which is essential to perform this method is provided.

Then this method is applied to a 2-D heat transfer problem using open-source software OpenFAOM. The result shows that this method could give optimization results on multi objects for example power dissipation and heat transfer. The results show that force coolant move close to high temperature is a method to enhance heat transfer. The highest heat transfer result is 67% higher than the lowest one, which proves this method to be practical.

In this article, the detailed derivation process of this method is provided in Sections 3.1 and 3.2, which may help other researchers who are interested in this method perform this kind of optimization more easily.

It also worth noting that the optimization results displayed in this article may not be global optima. Different optimization loop will get different optimal results. More research should be done to this method.

Acknowledgment

The authors would like to acknowledge the financial support from the National Natural Science Foundation of China Project (51676106).

ORCID

Bengt Sundén http://orcid.org/0000-0002-6068-0891

References

[1] M. P. Bendsoe and N. Kikuchi, "Generating optimal topologies in structural design using a homogenization method," *Comput. Methods Appl. Mech. Eng.*, vol. 71, no. 2, pp. 197–224, 1988. DOI: 10.1016/0045-7825(88)90086-2.

[2] M. Bendsoe and O. Sigmund, *Topology Optimization: Theory, Methods, and Applications*. Berlin, Heidelberg: Springer, 2004.

[3] T. Borrvall and J. Petersson, "Topology optimization of fluids in Stokes flow," *Int. J. Numer. Meth. Fluids*, vol. 41, no. 1, pp. 77–107, 2003. DOI: 10.1002/fld.426.

[4] O. Moos, F. Klimetzek, and R. Rossmann, "Bionic optimization of air-guiding systems," ASAE Technical Paper 2004-01-1377. 2004.

[5] C. Othmer, "Adjoint methods for car aerodynamics," *Math. Indus.*, vol. 4, no. 1, p. 6, 2014. DOI: 10.1186/2190-5983-4-6.

[6] A. Gersborg-Hansen, O. Sigmund, and R. Haber, "Topology optimization of channel flow problems," *Struct. Multidisc. Optim.*, vol. 30, no. 3, pp. 181–192, 2005. DOI: 10.1007/s00158-004-0508-7.

[7] C. Othmer and T. Grahs, "Approaches to fluid dynamic optimization in the car development process," Proceedings of the EUROGEN Conference, Munich, Germany, 2005.

[8] C. Othmer, "A continuous adjoint formulation for the computation of topological and surface sensitivities of ducted flows," *Int. J. Numer. Meth. Fluids*, vol. 58, no. 8, pp. 861–877, 2008. DOI: 10.1002/fld.1770.

[9] R. P. Dwight and J. Brezillon, "Effect of various approximations of the discrete adjoint on gradient-based optimization," AIAA-2006-0690, 2006. DOI: 10.2514/6.2006-690.

[10] E. M. Dede, "Multiphysics topology optimization of heat transfer and fluid flow system," Proceedings of the COMSOL Conference, Boston, 2009.

[11] E. A. Kontoleontos, E. M. Papoutsis-Kiachagias, A. S. Zymaris, D. I. Papadimitriou, and K. C. Giannakoglou, "Adjoint-based constrained topology optimization for viscous flows, including heat transfer," *Eng. Optim.*, vol. 45, no. 8, pp. 941–961, 2013. DOI: 10.1080/0305215X.2012.717074.

[12] T. Matsumori, T. Kondoh, A. Kawamoto, and T. Nomura, "Topology optimization for fluid-thermal interaction problems under constant input power," *Struct. Multidisc. Optim.*, vol. 47, no. 4, pp. 571–581, 2013. DOI: 10.1007/s00158-013-0887-8.

[13] G. Marck and Y. Privat, "On some shape and topology optimization problems in conductive and convective heat transfers," OPTI 2014, an International Conference on Engineering and Applied Sciences Optimization, M.G. Karlaftis and N.D. Lagaros, eds. 2014.

[14] G. Marck, M. Nemer, and J.-L. Harion, "Topology optimization of heat and mass transfer problems: Laminar flow," *Numer. Heat Transf., B: Fundam.*, vol. 63, no. 6, pp. 508–539, 2013. DOI: 10.1080/10407790.2013.772001.

[15] M. Pietropaoli, R. Ahlfeld, and F. Montomoli, "Design for additive manufacturing: Internal channel optimization," ASME Conference Paper, GT 57318, 2016. DOI: 10.1115/GT2016-57318.

[16] S. B. Dilgen, C. B. Dilgen, D. R. Fuhrman, O. Sigmund, and B. S. Lazarov, "Density based topology optimization of turbulent flow heat transfer systems," *Struct. Multidisc. Optim.*, vol. 57, no. 5, pp. 1905–1918, 2018. DOI: 10.1007/s00158-018-1967-6.

[17] K. Svanberg, "The Method of Moving Asymptotes—A new Method for Structural Optimization," *Int. J. Numer. Methods Eng.*, vol. 24, no. 2, pp. 359–373, 1987. DOI: 10.1002/nme.1620240207.